

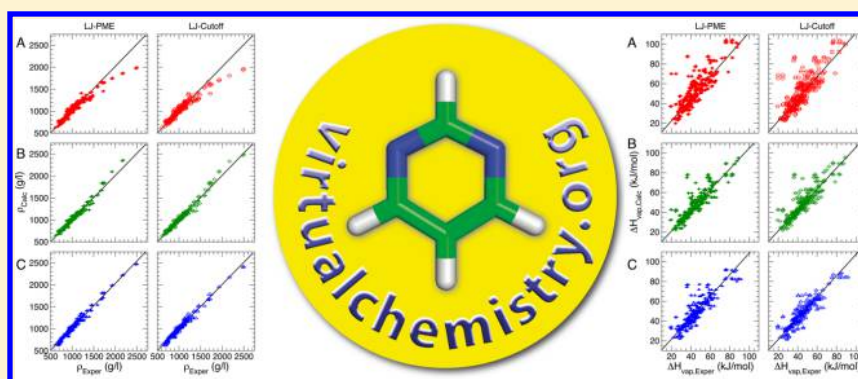
# Properties of Organic Liquids when Simulated with Long-Range Lennard-Jones Interactions

Nina M. Fischer,<sup>†</sup> Paul J. van Maaren,<sup>†</sup> Jonas C. Ditz,<sup>†</sup> Ahmet Yildirim,<sup>‡</sup> and David van der Spoel<sup>\*,†</sup>

<sup>†</sup>Uppsala Centre for Computational Chemistry, Science for Life Laboratory, Department of Cell and Molecular Biology, Uppsala University, Husargatan 3, Box 596, SE-75124 Uppsala, Sweden

<sup>‡</sup>Department of Physics, Faculty of Science and Art, Siirt University, 56100 Siirt, Turkey

**S** Supporting Information



**ABSTRACT:** In order to increase the accuracy of classical computer simulations, existing methodologies may need to be adapted. Hitherto, most force fields employ a truncated potential function to model van der Waals interactions, sometimes augmented with an analytical correction. Although such corrections are accurate for homogeneous systems with a long cutoff, they should not be used in inherently inhomogeneous systems such as biomolecular and interface systems. For such cases, a variant of the particle mesh Ewald algorithm (Lennard-Jones PME) was already proposed 20 years ago (Essmann et al. *J. Chem. Phys.* **1995**, *103*, 8577–8593), but it was implemented only recently (Wennberg et al. *J. Chem. Theory Comput.* **2013**, *9*, 3527–3537) in a major simulation code (GROMACS). The availability of this method allows surface tensions of liquids as well as bulk properties to be established, such as density and enthalpy of vaporization, without approximations due to truncation. Here, we report on simulations of  $\approx 150$  liquids (taken from a force field benchmark: Coleman et al. *J. Chem. Theory Comput.* **2012**, *8*, 61–74) using three different force fields and compare simulations with and without explicit long-range van der Waals interactions. We find that the density and enthalpy of vaporization increase for most liquids using the generalized Amber force field (GAFF, Wang et al. *J. Comput. Chem.* **2004**, *25*, 1157–1174) and the Charmm generalized force field (CGenFF, Vanommeslaeghe et al. *J. Comput. Chem.* **2010**, *31*, 671–690) but less so for OPLS/AA (Jorgensen and Tirado-Rives, *Proc. Natl. Acad. Sci. U.S.A.* **2005**, *102*, 6665–6670), which was parametrized with an analytical correction to the van der Waals potential. The surface tension increases by  $\approx 10^{-2}$  N/m for all force fields. These results suggest that van der Waals attractions in force fields are too strong, in particular for the GAFF and CGenFF. In addition to the simulation results, we introduce a new version of a web server, <http://virtualchemistry.org>, aimed at facilitating sharing and reuse of input files for molecular simulations.

## 1. INTRODUCTION

The predictive power of molecular simulation can be validated by comparing simulation results to experimental data. A large amount of accurate experimental data is available for molecular liquids; hence, these form a good source for benchmarking force fields used for molecular simulations.<sup>1,2</sup> Since the chemical composition of organic liquids is similar to moieties in biological systems, such as amino acids, benchmarks of force fields for organic liquids can serve as a proxy for force field benchmarks of biomolecules. In a previous paper, we tested the OPLS/AA<sup>3</sup> and GAFF<sup>4</sup> force fields for a set of 146 organic liquids.<sup>1</sup> The free energy of solvation of organic liquids in organic solvents was determined using thermodynamic

integration in an additional paper.<sup>2</sup> From these studies, we were able to find systematic issues, for instance, with charges for nitro groups in GAFF, since all molecules with that functional group have properties deviating from experiment. Another observation that we made was that the surface tension of simulated liquids was systematically underestimated. It was pointed out in a subsequent paper by Zubillaga and co-workers that the cutoff used for Lennard-Jones interactions was largely to blame for this finding.<sup>5</sup> They increased the Lennard-Jones cutoff from 1.1 nm used by Coleman and co-workers<sup>1</sup> to 2.3 nm

**Received:** February 26, 2015

**Published:** May 20, 2015



and obtained much better agreement with experimental data.<sup>5</sup> This observation does not come as a surprise, since the importance of van der Waals interactions for liquid properties like the enthalpies of vaporization had already been pointed out by MacKerell and Karplus in the early 1990s using Monte Carlo calculations.<sup>6</sup>

Allen and Tildesley introduced analytical corrections to Lennard-Jones cutoffs for spherical homogeneous systems.<sup>7</sup> These tail corrections apply as long as the liquid under study is unstructured beyond the cutoff, a condition that depends on the properties of the liquid under study (polarity, size of the molecules), on the temperature, and on the length of the cutoff. Analytical corrections for the effect of a cutoff in slab systems have been used by a number of groups as well.<sup>8–10</sup> The validity of such a correction is based on the same condition as for the spherical case, but ordering induced by the surface layer bordering the interface may make it more difficult for the condition to be met. More systematic methods have been proposed based on lattice sums.<sup>11–13</sup> Although the corresponding method for computing Coulomb interactions (particle mesh Ewald<sup>14</sup>) has been widely implemented in molecular simulation packages, the Lennard-Jones PME (LJ-PME) method has not been applied much.

The recent implementation<sup>15</sup> of this algorithm into the GROMACS package<sup>16,17</sup> may change this. In that work, a significant difference in properties of membranes including order parameters, area per lipid, and surface tension of phospholipid–water systems was found when the LJ-PME method was used. This demonstrates that the long-range ordering in such inherently inhomogeneous systems has a profound impact on the properties of the systems and that it is difficult to model the forces due to this ordering using cutoffs and analytical approximations.

For completeness, a number of other papers on algorithms for computing van der Waals interactions should be mentioned. Wu and Brooks introduced the isotropic periodic sum (IPS) method that approximates the long-range Coulomb or dispersion forces by assuming that atoms far away (beyond a certain cutoff distances) are arranged similarly to those that are closer.<sup>18</sup> The method is mathematically involved but computationally quite efficient. It has been applied to both homogeneous<sup>18</sup> and heterogeneous systems.<sup>19</sup> In the latter case, however, the method was combined with an Ewald summation method in order to deal with long-range inhomogeneity. The (Coulomb) IPS method was recently tested for liquid crystals and compared to Ewald summation.<sup>20</sup> In that work, it was demonstrated that two different phases of the liquid crystal were described quite well by the IPS method, but deviations were found close to the phase transition.

In principle, simulation results should become more accurate when systematic errors (i.e., cutoffs) are removed. For instance, layering artifacts are induced in water boxes when the cutoff length fits an integer number of times in the computational box.<sup>21</sup> This effect was shown to disappear when using long-range electrostatics methods.<sup>22</sup> Here, by applying the LJ-PME method, we can verify whether the Lennard-Jones cutoff of 1.1 nm that we used previously in combination with an analytical correction<sup>1</sup> yields different liquid properties than a treatment without cutoffs. As we will show below, there is a large effect on the surface tension, in line with the work of Zubillaga and colleagues.<sup>5</sup> We realize that most force fields were developed with a specific cutoff for Lennard-Jones interactions and hence the ad hoc introduction of the LJ-PME method will not

automatically yield observables closer to experimental data. However, the purpose of this work is solely to quantify the changes in observables due to introduction of the LJ-PME algorithm.

In this work, we re-evaluate the properties of the organic liquids that we studied previously<sup>1</sup> using the LJ-PME implementation<sup>15</sup> in the GROMACS simulation software.<sup>17</sup> For all molecules, topologies were generated for the Charmm generalized force field (CGenFF)<sup>23,24</sup> in addition to the earlier mentioned OPLS/AA<sup>3</sup> and GAFF.<sup>4</sup>

One complication arises from the usage of combination rules for  $\sigma$  and  $\epsilon$  in the Lennard-Jones potential

$$V_{ij}(r_{ij}) = 4\epsilon_{ij} \left[ \left( \frac{\sigma_{ij}}{r_{ij}} \right)^{12} - \left( \frac{\sigma_{ij}}{r_{ij}} \right)^6 \right] = \frac{A_{ij}}{r_{ij}^{12}} - \frac{B_{ij}}{r_{ij}^6} \quad (1)$$

where  $r_{ij}$  is the distance between atoms  $i$  and  $j$ ,  $\sigma_{ij}$  is the combined van der Waals radius, and  $\epsilon_{ij}$  is the depth of the potential well. For efficiency reasons, the LJ-PME method is practical only<sup>15</sup> when geometric combination rules are used that have the form

$$B_{ii} = 4\epsilon_{ii}\sigma_{ii}^6, \quad B_{ij} = \sqrt{B_{ii}B_{jj}} \quad (2)$$

OPLS/AA uses this combination rule, but GAFF and CGenFF use the Lorentz–Berthelot rules

$$\sigma_{ij} = \frac{1}{2}(\sigma_{ii} + \sigma_{jj}), \quad \epsilon_{ij} = \sqrt{\epsilon_{ii}\epsilon_{jj}} \quad (3)$$

Wennberg and co-workers estimate that the difference is negligible in practice and that the error induced by changing the combination rules (which affects only the long-range part of the potential) is much less than the error due to truncation.<sup>15</sup>

## 2. METHODS

**2.1. Molecular Models.** The liquid models based on GAFF and OPLS/AA are taken from <http://virtualchemistry.org>, except for 21 of the OPLS/AA models for which we corrected some topology errors (see Supporting Information for a detailed list). The CGenFF topologies were generated based on the GAFF PDB files from Coleman and co-workers.<sup>1</sup> Openbabel<sup>25</sup> was used to convert these PDB files into MOL2 files that subsequently were uploaded to the Paramchem server (<http://cgenff.paramchem.org>).<sup>24</sup> This server (using version 0.9.7 beta of the CGenFF program) provides Toppar stream files (STR) for use with CGenFF, version 2b8. These STR files have been converted to GROMACS topologies using a modified version of the `charmm2gromacs.py` script.

**2.2. Simulation Details.** The GROMACS simulation package<sup>16,17</sup> (version 4.5) was used for all simulations. The data simulated with a Lennard-Jones potential cutoff at 1.1 nm and a long-range analytical dispersion correction<sup>7</sup> for both OPLS/AA and GAFF force fields was taken from Coleman and co-workers<sup>1</sup> (except for the 21 molecules with corrected OPLS/AA topologies). A discussion of how cutoffs are used in some of the main simulation codes (and accompanying force fields) was given by van der Spoel and van Maaren.<sup>22</sup> For the CGenFF force field, the simulations using the Lennard-Jones potential cutoff (including dispersion corrections) were performed in the same manner as that for the simulations of the 21 molecules with corrected OPLS/AA topologies, as described in Coleman and co-workers<sup>1</sup> and briefly in the following.

For bulk liquid simulations (named LIQ below) as well as surface tension simulations (named SURF), the particle mesh Ewald (PME) method was used to treat Coulomb interactions with a switching distance of 1.1 nm. The Nosé–Hoover<sup>26,27</sup> algorithm was applied for temperature coupling in order to ensure correct temperature fluctuations. For production simulations at constant pressure, we used the Parrinello–Rahman pressure coupling<sup>28</sup> algorithm with the compressibility set to  $5 \times 10^{-5} \text{ bar}^{-1}$  and the time constant set to 5 ps. In all simulations, bonds were constrained using the LINCS<sup>29,30</sup> algorithm. For the SURF simulations, corrections to the electrostatics for slab systems were applied.<sup>31</sup> For all three force fields, separate gas-phase simulations (named GAS) were run, without any cutoff in order to be able to extract the enthalpy of vaporization. LIQ and SURF production simulations were 10 ns, whereas the GAS production simulations were 100 ns.

New production simulations were performed for the three force fields using the Lennard-Jones PME method<sup>12</sup> instead of a potential cutoff for bulk liquid and surface tension simulations. All other simulation parameters remained the same. We indicate these three force fields as GLJPME (GAFF/LJ-PME), OLJPME (OPLS/AA/LJ-PME), and CLJPME (CGenFF/LJ-PME). Complete molecular topologies and structures for use with the GROMACS software suite as well as equilibrated liquid boxes containing coordinates for all systems are available from our website <http://virtualchemistry.org>.

### 3. RESULTS

**3.1. Equilibration.** All properties, surface tension, density, etcetera were calculated over the last 9 ns for LIQ and SURF simulations and for 90 ns for GAS simulations. Obtaining equilibrium properties takes longer in GAS simulations because the energies are not averaged over many molecules. Some of the simulations were extended a number of times until the energy convergence criterion was reached either in the last 9 ns (LIQ, SURF) or 90 ns (GAS), being that the drift in the total energy of these production simulations was at most 0.5 J/mol/ns per degree of freedom. Most simulations fulfilled this criterion during the first production simulation, but some simulations had to be extended to reach convergence.

**3.2. Algorithmic Properties.** In order to illustrate the effect of LJ-PME on liquid properties, 5 ns simulations of 1-bromopropane were performed using the OPLS/AA force field<sup>3</sup> with varying cutoffs (the Fourier grid spacing was scaled linearly with the cutoff). LJ-PME was compared to a dispersion correction and to a plain cutoff (Figure 1). Energy and density are essentially constant from a cutoff of 0.8 nm onward for LJ-PME and from 1.0 nm for dispersion correction. The simulations using a plain cutoff do not converge at all, although a fit of the total energy to a function  $y = E_0 + E_1x^{-3}$  yields an asymptotic value of  $E_0 = 25.7 \text{ kJ/mol}$ , virtually identical to the LJ-PME value. A similar fit to the density yields an asymptotic value of 1430 g/L, which is somewhat higher than the LJ-PME value (1408 g/L). Finally, the additional CPU time needed for the LJ-PME is significant at  $\approx 45\%$  for cutoffs larger than 1.1 nm.

**3.3. Surface Tension.** The surface tension of liquids is expected to differ significantly upon introducing long-range Lennard-Jones interactions. Figure 2 shows that this is indeed the case and that most systems yield a higher surface tension. Some of the liquids did not remain liquid in these simulations and, therefore, display a negative surface tension (those liquids

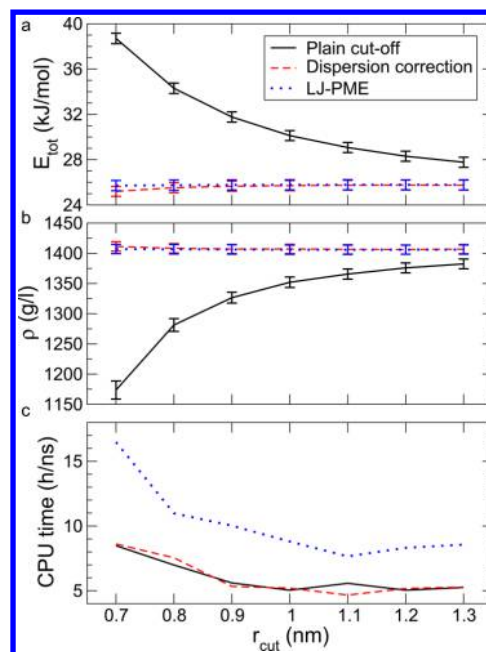


**Figure 1.** (A) Total energy, (B) density, and (C) CPU time used as a function of cutoff in simulations of 1-bromopropane in the bulk using the OPLS/AA force field.

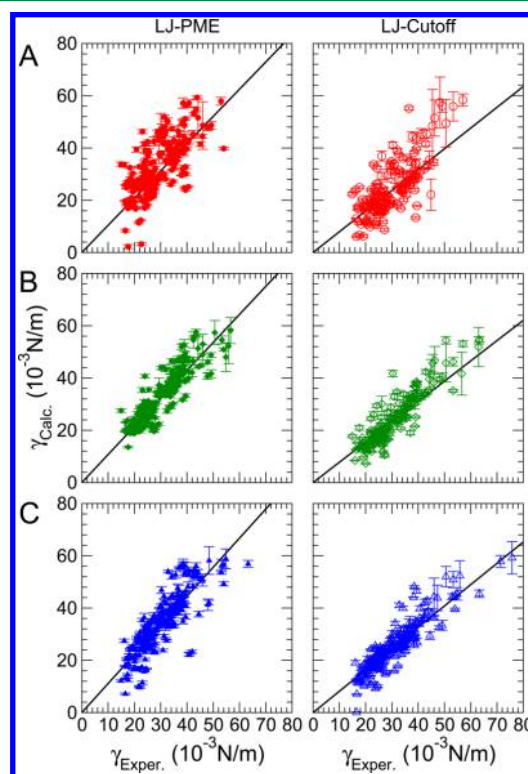


**Figure 2.** Correlation between surface tension ( $\gamma$ ) calculated by MD simulation using (A) GAFF, (B) OPLS/AA, and (C) CGenFF and experiment. Simulations using either Lennard-Jones PME or cutoff. The slopes of the lines are given in Table 1.

are not shown in Figure 2 but are listed in Table S5). This, in practice, means that the models have a boiling point that is too low. The line drawn in each of the panels of the figure is due to a regression analysis to  $y = ax$  (Table 1). The slope of these



lines is larger than 1 for simulations with LJ-PME and considerably smaller than 1 for simulations with a cutoff.

**Table 1. Statistics of a Linear Fit of Calculated to Experimental Values According to  $y = ax^a$**

force field	N	a	RMSD	% dev	R <sup>2</sup>
$\rho$ (g/L)					
GLJPME	265	1.01	87.4	5	94%
GAFF	187	1.01	88.5	5	93%
OLJPME	248	1.01	43.0	3	98%
OPLS	185	1.01	43.6	3	98%
CLJPME	243	1.01	39.5	3	98%
CGenFF	148	1.00	38.8	3	97%
$\Delta H_{\text{vap}}$ (kJ/mol)					
GLJPME	371	1.12	12.5	20	66%
GAFF	272	1.12	12.4	19	62%
OLJPME	345	1.05	7.2	10	70%
OPLS	255	1.06	8.1	11	74%
CLJPME	330	1.09	8.3	13	75%
CGenFF	197	1.07	6.6	11	80%
$\gamma$ (10 <sup>-3</sup> N/m)					
GLJPME	237	1.04	7.9	20	45%
GAFF	165	0.77	8.6	24	46%
OLJPME	210	1.07	5.4	14	78%
OPLSZ	56	1.05	5.4	13	60%
OPLS	169	0.76	7.8	22	73%
CLJPME	250	1.11	7.2	19	71%
CGenFF	199	0.82	7.0	20	76%
$\epsilon(0)$					
GLJPME	237	0.61	6.6	34	83%
GAFF	170	0.61	6.9	35	83%
OLJPME	247	0.49	10.1	44	67%
OPLS	175	0.51	9.0	44	66%
CLJPME	233	0.39	8.5	44	46%
CGenFF	134	0.39	8.6	44	44%
$\alpha_p$ (10 <sup>-3</sup> /K)					
GLJPME	296	1.09	0.3	19	52%
GAFF	164	1.10	0.3	21	39%
OLJPME	259	1.14	0.3	20	64%
OPLS	171	1.15	0.3	21	59%
CLJPME	274	1.14	0.3	19	55%
CGenFF	156	1.12	0.3	16	56%
$\kappa_T$ (1/GPa)					
GLJPME	172	0.80	0.3	25	61%
GAFF	122	0.80	0.3	27	51%
OLJPME	154	0.97	0.2	14	80%
OPLS	120	0.96	0.2	15	71%
CLJPME	157	0.90	0.2	16	70%
CGenFF	100	0.91	0.2	17	70%

<sup>a</sup>Uncertainties in the simulation results are used as weights in the fit. The number of (experimental) data points  $N$  is given for each property. Root-mean-square deviation (RMSD) is from experimental values, average deviation is given in percent, and the coefficient of determination  $R^2$  is given.

**3.4. Other Properties.** Table 1 lists the predictive power for the liquid density  $\rho$ , the enthalpy of vaporization  $\Delta H_{\text{vap}}$ , the surface tension  $\gamma$ , the dielectric constant  $\epsilon_0$ , the isothermal compressibility  $\kappa_T$ , and the volumetric expansion coefficient  $\alpha_p$  (note that Table 2 in Coleman and co-workers<sup>1</sup> lists  $R^2$ ; however, the values given correspond to  $R$  instead). All of the

analysis methods used date back to the 1980s<sup>7,32</sup> and therefore we refer to Coleman et al. for details.<sup>1</sup>

CGenFF and OPLS/AA perform somewhat better (as judged from the root-mean-square deviation from experiment) than GAFF for  $\rho$ ,  $\Delta H_{\text{vap}}$ , and  $\gamma$ , but, interestingly, the reverse is true for  $\epsilon_0$ . A table showing the average relative deviation per molecule (how well the force field performs for a specific molecule, relative to the performance of the force field as a whole) is given in the Supporting Information (Table S2). In addition to systematic issues mentioned by Coleman and co-workers,<sup>1</sup> we find that CGenFF has problems with amine groups, as 1,2-diaminoethane, propan-1-amine, and propan-2-amine have relatively large deviation from experiment due to too low density and negative surface tension. Interestingly, the negative surface tension turns into positive for propan-1-amine when using LJ-PME, highlighting that subtle changes in the energy function can have a significant effect on molecular properties.

**3.5. Net Effect of LJ-PME on Liquid Properties.** Table 2 shows the average change (over molecules) for six liquid properties (note that here, too, the negative surface tensions are not taken into account). The surface tension increases by  $\approx 0.01$  N/m for all force fields due to improved ordering. For OPLS/AA, the increase in  $\gamma$  is similar to that for the other force fields because one can not use a spherical analytical correction for a cutoff for a slab system. As noted above, the analytical correction proposed by Sun and colleagues might provide an efficient alternative for homogeneous slab systems,<sup>10</sup> but this was not employed here. Both density and enthalpy of vaporization increase for GAFF and CGenFF when LJ-PME is used, showing that the dispersion forces stabilize the liquid state in these force fields. Although the standard deviations in the differences are relatively large (Table 2), they are considerably smaller than those in the properties themselves (Table 1), strongly suggesting that the differences are statistically significant.

The structure of the liquids can be studied using the total radial distribution function

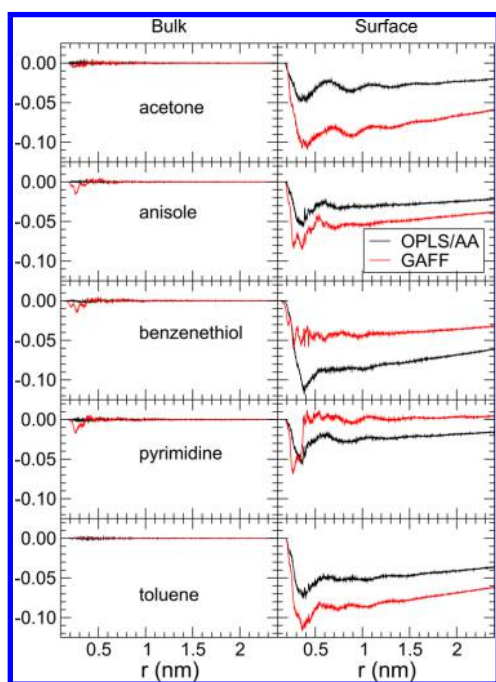
$$g(r) = \sum_{i \neq j} \frac{\delta(r - r_{ij})}{4\pi r^2} \quad (4)$$

The difference in liquid structure induced by the introduction of long-range Lennard-Jones interactions is illustrated for five molecules in Figure 3 that shows  $\Delta g(r) = g_{\text{cut-off}}(r) - g_{\text{LJ-PME}}(r)$ . It is clear that for OPLS/AA the bulk structure hardly changes, since the difference between the use of dispersion correction and LJ-PME is small. For GAFF, we find that the density increases by 8 g/L, on average, due to LJ-PME. It can be seen that the main structural rearrangements occur at short distance; thus, the packing becomes tighter ( $\Delta g(r)$  less than zero, indicating that the peaks in the  $g(r)$  function are higher for the LJ-PME simulations). According to a review by Chandler and colleagues,<sup>33</sup> long-range van der Waals forces have little effect on the structure of liquids at short range. We find that this effect is small but not negligible (Figure 3) and mainly noticeable at short distances. For the surface tension simulations, the effects are much larger, since we move from a plain cutoff to LJ-PME. Here as well, the change in packing at short distance is the most obvious effect caused by LJ-PME.

**3.6. Updated virtualchemistry.org Website.** With our previous benchmark paper,<sup>1</sup> we introduced a web server that allows other workers to download the molecular topologies and

Table 2. Average Change in Properties for Molecular Liquids upon Introducing LJ-PME and Standard Deviation in the Change<sup>a</sup>

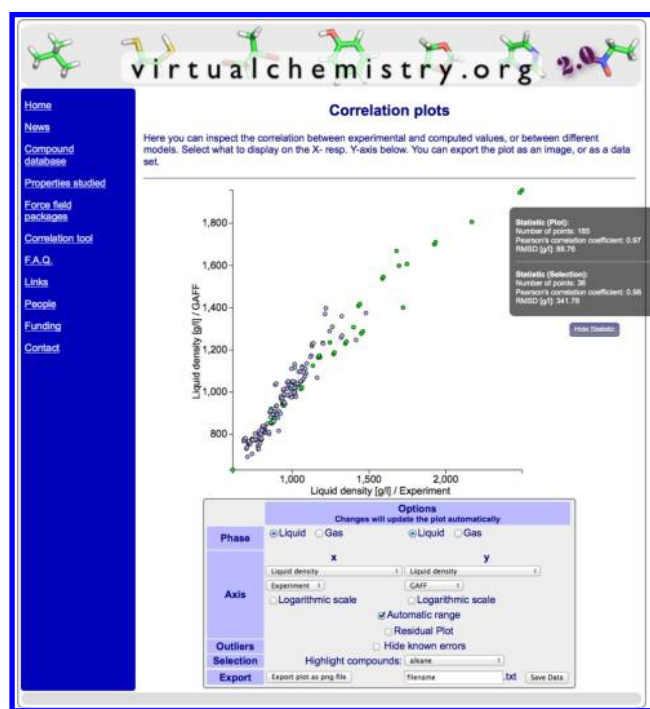
property	GAFF	OPLS	CGenFF
$\Delta\rho$ (g/L)	$8 \pm 14$ (236)	$2 \pm 8$ (212)	$12 \pm 15$ (187)
$\Delta\Delta H_{\text{vap}}$ (kJ/mol)	$0.5 \pm 1.0$ (227)	$-0.2 \pm 1.1$ (200)	$0.3 \pm 1.2$ (179)
$\Delta\gamma$ (0.001 N/m)	$9 \pm 10$ (144)	$10 \pm 10$ (132)	$10 \pm 10$ (209)
$\Delta\epsilon_0$	$0.2 \pm 3.0$ (166)	$0.3 \pm 3.3$ (168)	$0.0 \pm 1.1$ (147)
$\Delta\alpha_p$ (0.001/K)	$0.0 \pm 0.2$ (234)	$-0.0 \pm 0.1$ (208)	$0.0 \pm 0.1$ (187)
$\Delta\kappa_T$ (1/GPa)	$0.0 \pm 0.1$ (234)	$-0.0 \pm 0.1$ (208)	$0.0 \pm 0.1$ (187)

<sup>a</sup>Values in brackets refer to the number of data points.Figure 3. Change in liquid structure  $\Delta g(r)$  for bulk simulations (bulk) and those with a liquid–vapor interface (surface) for five liquids for five molecules and two force fields.

coordinates in order to reproduce and extend our work.<sup>34</sup> This web server has been completely redesigned to make it more future proof, but it also offers new functionality, like user-defined correlation plots between data sets (Figure 4), with the option of downloading such plots as graphic images for use in presentations or as data sets.

#### 4. DISCUSSION

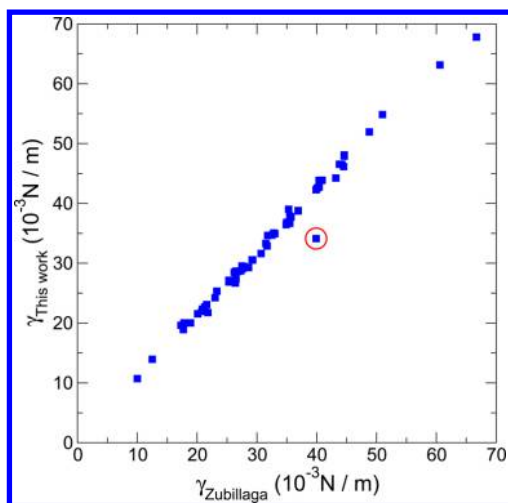
The surface tension as well as other properties of molecular liquids was computed using molecular simulations. It was shown that inclusion of long-range Lennard-Jones interactions increases the surface tension independent of the underlying force field (Figure 2); the slope in a regression analysis comparing computed to experimental  $\gamma$  changes from  $\approx 0.8$  to  $\approx 1.1$  for all three force fields. This is expected since the LJ-PME algorithm adds only attractive interactions. The fact that, without a cutoff, all force fields now overestimate the surface tension indicates that the dispersion interactions are too strong in all of the used force fields. Since the potential functions for GAFF and CGenFF were developed with cutoffs, whereas OPLS/AA was developed with an analytical correction,<sup>3,22</sup> it seems that there is an implicit overcompensation in the GAFF and CGenFF parameters for missing out on the all-attractive dispersion interactions. The finding that even OPLS/AA

Figure 4. Screen shot of the <http://virtualchemistry.org> website, showing a correlation plot.

displays a systematically too high surface tension with LJ-PME suggests that the structure of the liquid is not homogeneous at 1.1 nm, the cutoff used when not applying LJ-PME, and hence that the analytical corrections to pressure and energy<sup>7</sup> are valid only when using an even longer cutoff. This is visible in the radial distribution functions for some of the liquids (Figure 3).

Zubillaga and co-workers tested the convergence of the surface tension and the liquid density of four liquids with increasing cutoff. They found that at 2.3 nm the result converged.<sup>5</sup> This is double the cutoff used by Coleman and co-workers and much longer than what is customarily used, although the need for a long cutoff could be more serious due to the presence of an interface. The surface tension results using this long cutoff are virtually identical to the ones computed using LJ-PME (Figure 5) except for some molecules where we used an updated topology. According to the benchmarks performed by Wennberg and colleagues,<sup>15</sup> LJ-PME is almost as efficient as a cutoff of 1.6 nm and, therefore, LJ-PME is a better choice than a long cutoff for efficiency reasons as well as for accurate calculation of long-range interactions.

Some caution when computing surface tension in finite size systems is necessary. A number of studies have evaluated the



**Figure 5.** Correlation between surface tension computed using the OPLS/AA force field with a long cutoff of 2.3 nm on the  $x$ -axis (numbers taken from ref 5) and LJ-PME ( $y$ -axis). The outlier in the red ring is thiophene, where, in our new simulations, the Lennard-Jones parameters of the sulfur atom were corrected.

effect of system size on the surface tension and other properties for Lennard-Jones fluids. Orea et al. used Lennard-Jones lattice sum methods and found that for a system size larger than 7 to 8 molecular lengths the surface tension is converged.<sup>35</sup> Janaček used an analytical correction for slab systems when studying Lennard-Jones fluids<sup>8,9</sup> and concluded the same. Since we used boxes of  $10 \times 10 \times 10$  molecules, the size is sufficiently large such that the surface tension should be converged.

The notion that the dispersion forces are systematically too strong could affect, for instance, the stability of proteins in molecular dynamics simulations. Since proteins have a higher density than water, the Lennard-Jones interactions between protein atoms will be artificially too strong, which may lead to overstabilization of folded protein structures. The thermodynamic stability of proteins is only marginal at best, typically around  $\Delta G_{\text{unfold}} \approx 40$  kJ/mol; for experimental numbers, see the work of, e.g., Kim et al.<sup>36</sup> and Chrnyk et al.,<sup>37</sup> and for a database of stabilities, see the work of Bava et al.<sup>38</sup> Molecular simulations trying to quantify the Gibbs energy of folding yield numbers in the right order of magnitude.<sup>39–42</sup> The influence of different force fields on simulating proteins has been examined before,<sup>43–45</sup> and differences between force fields are apparent. Here, we conclude that a reoptimization of force fields using LJ-PME should be attempted in order to remove artifacts due to the fact that protein force fields were implicitly adjusted to the use of a Lennard-Jones cutoff. Such an endeavor may breathe yet some more new life into these third-generation force fields, but it is also needed for more modern polarizable force fields.<sup>46,47</sup> The added computational cost in the present implementation in GROMACS is about 45% using a 1.1 nm cutoff (Figure 1), which does not seem unreasonable in order to obtain results that are independent of changes in the cutoff (Figure 1). The most objective manner to evaluate such force field adaptations seems to be by benchmarking the properties of molecular liquids.<sup>1,2</sup>

## ■ ASSOCIATED CONTENT

### Supporting Information

Additional figures showing correspondence between experimental and simulated properties as well as tables with all data,

including reference experimental values. The Supporting Information is available free of charge on the ACS Publications website at DOI: 10.1021/acs.jctc.5b00190.

## ■ AUTHOR INFORMATION

### Corresponding Author

\*E-mail: david.vanderspoel@icm.uu.se.

### Funding

The Swedish research council is acknowledged for financial support to D.v.d.S. (grant 2013-5947) and for a grant of computer time (SNIC2013-26-6) through the High Performance Computing Center North in Umeå, Sweden. N.M.F. is supported through eSENCE—The e-Science Collaboration (Uppsala-Lund-Umeå, Sweden).

### Notes

The authors declare no competing financial interest.

## ■ REFERENCES

- (1) Caleman, C.; van Maaren, P. J.; Hong, M.; Hub, J. S.; Costa, L. T.; van der Spoel, D. *J. Chem. Theory Comput.* **2012**, *8*, 61–74.
- (2) Zhang, J.; Tuguldur, B.; van der Spoel, D. *J. Chem. Inf. Model.* DOI: 10.1021/acs.jcim.5b00106.
- (3) Jorgensen, W. L.; Tirado-Rives, J. *Proc. Natl. Acad. Sci. U.S.A.* **2005**, *102*, 6665–6670.
- (4) Wang, J.; Wolf, R. M.; Caldwell, J. W.; Kollman, P. A.; Case, D. A. *J. Comput. Chem.* **2004**, *25*, 1157–1174.
- (5) Zubillaga, R. A.; Labastida, A.; Cruz, B.; Martínez, J. C.; Sánchez, E.; Alejandre, J. *J. Chem. Theory Comput.* **2013**, *9*, 1611–1615.
- (6) MacKerell, A. D.; Karplus, M. *J. Phys. Chem.* **1991**, *95*, 10559–10560.
- (7) Allen, M. P.; Tildesley, D. J. *Computer Simulation of Liquids*; Oxford Science Publications: Oxford, 1987.
- (8) Janaček, J. *J. Phys. Chem. B* **2006**, *110*, 6264–6269.
- (9) Janaček, J. *J. Chem. Phys.* **2009**, *131*, 124513.
- (10) Sun, L.; Li, X.; Hede, T.; Tu, Y.; Leck, C.; Agren, H. *J. Phys. Chem. B* **2012**, *116*, 31983204.
- (11) Karasawa, N.; Goddard, W. A., III *J. Phys. Chem.* **1989**, *93*, 7320–7327.
- (12) Essmann, U.; Perera, L.; Berkowitz, M. L.; Darden, T.; Lee, H.; Pedersen, L. G. *J. Chem. Phys.* **1995**, *103*, 8577–8592.
- (13) Chen, Z.-M.; Gain, T.; Goddard, W. A., III *J. Comput. Chem.* **1997**, *18*, 1365–1370.
- (14) Darden, T.; York, D.; Pedersen, L. *J. Chem. Phys.* **1993**, *98*, 10089–10092.
- (15) Wennberg, C. L.; Murtola, T.; Hess, B.; Lindahl, E. *J. Chem. Theory Comput.* **2013**, *9*, 3527–3537.
- (16) Hess, B.; Kutzner, C.; Van der Spoel, D.; Lindahl, E. *J. Chem. Theory Comput.* **2008**, *4*, 435–447.
- (17) Pronk, S.; Páll, S.; Schulz, R.; Larsson, P.; Bjelkmar, P.; Apostolov, R.; Shirts, M. R.; Smith, J. C.; Kasson, P. M.; van der Spoel, D.; Hess, B.; Lindahl, E. *Bioinformatics* **2013**, *29*, 845–854.
- (18) Wu, X.; Brooks, B. R. *J. Chem. Phys.* **2005**, *122*, 044107.
- (19) Wu, C.; Wang, Z.; Lei, H.; Duan, Y.; Bowers, M. T.; Shea, J.-E. *J. Mol. Biol.* **2008**, *384*, 718–729.
- (20) Nozawa, T.; Takahashi, K. Z.; Kameoka, S.; Narumi, T.; Yasuoka, K. *Mol. Simul.* **2015**, DOI: 10.1080/08927022.2014.998210.
- (21) Yonetani, Y. *Chem. Phys. Lett.* **2005**, *406*, 49–53.
- (22) van der Spoel, D.; van Maaren, P. J. *J. Chem. Theory Comput.* **2006**, *2*, 1–11.
- (23) Vanommeslaeghe, K.; Hatcher, E.; Acharya, C.; Kundu, S.; Zhong, S.; Shim, J.; Darian, E.; Guvench, O.; Lopes, P.; Vorobyov, I.; Mackerell, A. D. *J. Comput. Chem.* **2010**, *31*, 671–690.
- (24) Vanommeslaeghe, K.; MacKerell, A. D. *J. Chem. Inf. Model.* **2012**, *52*, 3144–3154.
- (25) O’Boyle, N. M.; Banck, M.; James, C. A.; Morley, C.; Vandermeersch, T.; Hutchison, G. R. *J. Cheminf.* **2011**, *3*, 33.
- (26) Nosé, S. *Mol. Phys.* **1984**, *52*, 255–268.

- (27) Hoover, W. G. *Phys. Rev. A* **1985**, *31*, 1695–1697.
- (28) Parrinello, M.; Rahman, A. *J. Appl. Phys.* **1981**, *52*, 7182–7190.
- (29) Hess, B. *J. Chem. Theory Comput.* **2008**, *4*, 116–122.
- (30) Hess, B.; Bekker, H.; Berendsen, H. J. C.; Fraaije, J. G. E. M. *J. Comput. Chem.* **1997**, *18*, 1463–1472.
- (31) Yeh, I.-C.; Berkowitz, M. L. *J. Chem. Phys.* **1999**, *111*, 3155–3162.
- (32) Neumann, M. *Mol. Phys.* **1983**, *50*, 841–858.
- (33) Chandler, D.; Weeks, J. D.; Andersen, H. C. *Science* **1983**, *220*, 787–794.
- (34) van der Spoel, D.; van Maaren, P. J.; Caleman, C. *Bioinformatics* **2012**, *28*, 752–753.
- (35) Orea, P.; López-Lemus, J.; Alejandre, J. *J. Chem. Phys.* **2005**, *123*, 114702.
- (36) Kim, K. S.; Tao, F.; Fuchs, J.; Danishefsky, A. T.; Housset, D.; Wlodawer, A.; Woodward, C. *Protein Sci.* **1993**, *2*, 588–596.
- (37) Chrnyk, B. A.; Evans, J.; Lillquist, J.; Young, P.; Wetzel, R. *J. Biol. Chem.* **1993**, *268*, 18053–18061.
- (38) Bava, K. A.; Gromiha, M. M.; Uedaira, H.; Kitajima, K.; Sarai, A. *Nucl. Acid Res.* **2004**, *32*, D120–D121.
- (39) Seibert, M.; Patriksson, A.; Hess, B.; van der Spoel, D. *J. Mol. Biol.* **2005**, *354*, 173–183.
- (40) van der Spoel, D.; Seibert, M. M. *Phys. Rev. Lett.* **2006**, *96*, 238102.
- (41) Piana, S.; Lindorff-Larsen, K.; Shaw, D. E. *Proc. Natl. Acad. Sci. U.S.A.* **2012**, *109*, 17845–17850.
- (42) Jimenez-Cruz, C. A.; Garcia, A. E. *Phys. Chem. Chem. Phys.* **2014**, *16*, 6422–6429.
- (43) van der Spoel, D.; Lindahl, E. *J. Phys. Chem. B* **2003**, *107*, 11178–11187.
- (44) Lange, O. F.; van der Spoel, D.; de Groot, B. L. *Biophys. J.* **2010**, *99*, 647–655.
- (45) Piana, S.; Lindorff-Larsen, K.; Shaw, D. E. *Biophys. J.* **2011**, *100*, L47–L49.
- (46) Ponder, J. W.; Wu, C.; Ren, P.; Pande, V. S.; Chodera, J. D.; Schnieders, M. J.; Haque, I.; Mobley, D. L.; Lambrecht, D. S.; DiStasio, R. A., Jr.; Head-Gordon, M.; Clark, G. N. I.; Johnson, M. E.; Head-Gordon, T. *J. Phys. Chem. B* **2010**, *114*, 2549–2564.
- (47) Lopes, P. E. M.; Huang, J.; Shim, J.; Luo, Y.; Li, H.; Roux, B.; MacKerell, J.; Alexander, D. *J. Chem. Theory Comput.* **2013**, *9*, 5430–5449.